

ICES REPORT 12-04

January 2012

A Simple Algorithm for Obtaining Nearly Optimal Quadrature Rules for NURBS-based Isogeometric Analysis

by

F. Auricchio, F. Calabro, T.J.R. Hughes, A. Reali, and G. Sangalli



The Institute for Computational Engineering and Sciences
The University of Texas at Austin
Austin, Texas 78712

Reference: F. Auricchio, F. Calabro, T.J.R. Hughes, A. Reali, and G. Sangalli, A Simple Algorithm for Obtaining Nearly Optimal Quadrature Rules for NURBS-based Isogeometric Analysis, ICES REPORT 12-04, The Institute for Computational Engineering and Sciences, The University of Texas at Austin, January 2012.

Report Documentation Page

Form Approved
OMB No. 0704-0188

Public reporting burden for the collection of information is estimated to average 1 hour per response, including the time for reviewing instructions, searching existing data sources, gathering and maintaining the data needed, and completing and reviewing the collection of information. Send comments regarding this burden estimate or any other aspect of this collection of information, including suggestions for reducing this burden, to Washington Headquarters Services, Directorate for Information Operations and Reports, 1215 Jefferson Davis Highway, Suite 1204, Arlington VA 22202-4302. Respondents should be aware that notwithstanding any other provision of law, no person shall be subject to a penalty for failing to comply with a collection of information if it does not display a currently valid OMB control number.

1. REPORT DATE JAN 2012		2. REPORT TYPE		3. DATES COVERED 00-00-2012 to 00-00-2012	
4. TITLE AND SUBTITLE A Simple Algorithm for Obtaining Nearly Optimal Quadrature Rules for NURBS-based Isogeometric Analysis				5a. CONTRACT NUMBER	
				5b. GRANT NUMBER	
				5c. PROGRAM ELEMENT NUMBER	
6. AUTHOR(S)				5d. PROJECT NUMBER	
				5e. TASK NUMBER	
				5f. WORK UNIT NUMBER	
7. PERFORMING ORGANIZATION NAME(S) AND ADDRESS(ES) University of Texas at Austin, Institute for Computational Engineering and Sciences, Austin, TX, 78712				8. PERFORMING ORGANIZATION REPORT NUMBER	
9. SPONSORING/MONITORING AGENCY NAME(S) AND ADDRESS(ES)				10. SPONSOR/MONITOR'S ACRONYM(S)	
				11. SPONSOR/MONITOR'S REPORT NUMBER(S)	
12. DISTRIBUTION/AVAILABILITY STATEMENT Approved for public release; distribution unlimited					
13. SUPPLEMENTARY NOTES					
14. ABSTRACT We develop new quadrature rules for Isogeometric Analysis based on the solution of a local nonlinear problem. A simple and robust algorithm is developed to determine the rules which are exact for important B-Spline spaces of uniform and geometrically stretched knot spacings. We consider both periodic and open knot vector configurations and illustrate the efficiency of the rules on selected boundary value problems. We find that the rules are almost optimally efficient, but much easier to obtain than optimal rules, which require the solution of global nonlinear problems that are often ill-posed.					
15. SUBJECT TERMS					
16. SECURITY CLASSIFICATION OF:			17. LIMITATION OF ABSTRACT	18. NUMBER OF PAGES	19a. NAME OF RESPONSIBLE PERSON
a. REPORT unclassified	b. ABSTRACT unclassified	c. THIS PAGE unclassified			

A Simple Algorithm for Obtaining Nearly Optimal Quadrature Rules for NURBS-based Isogeometric Analysis

F. Auricchio^{a,b}, F. Calabrò^c, T.J.R. Hughes^d, A. Reali^{a,b}, G. Sangalli^{e,b}

^a *Dipartimento di Meccanica Strutturale, Università degli Studi di Pavia*

^b *Istituto di Matematica Applicata e Tecnologie Informatiche “E. Magenes” del CNR, Pavia*

^c *DAEIMI, Università degli Studi di Cassino*

^d *Institute for Computational Engineering and Sciences, University of Texas at Austin*

^e *Dipartimento di Matematica, Università degli Studi di Pavia*

Abstract

We develop new quadrature rules for Isogeometric Analysis based on the solution of a local nonlinear problem. A simple and robust algorithm is developed to determine the rules which are exact for important B-Spline spaces of uniform and geometrically stretched knot spacings. We consider both periodic and open knot vector configurations and illustrate the efficiency of the rules on selected boundary value problems. We find that the rules are almost optimally efficient, but much easier to obtain than optimal rules, which require the solution of global nonlinear problems that are often ill-posed.

Keywords: Numerical integration, Isogeometric analysis, NURBS, B-splines

1. Introduction

Isogeometric analysis (IGA) is a recently proposed computational technique [19] for the solution of boundary value problems, based on the idea of using the same functions adopted in Computer Aided Design (CAD) not only to describe the domain geometry, but also to build the numerical approximation of the problem solution.

In CAD a common choice for the representation of complex geometries is Non-Uniform Rational B-Splines (NURBS). Thus, a particular case of isogeometric methods is to represent the geometry, project the data, and find the solution in the space of NURBS. For the interested reader, we recall that IGA has been summarized in a recent book [13], studied in a number of contributions (e.g., [2, 4, 7, 14, 16, 17, 20]), and that it is having a progressively growing impact on fields as diverse as fluid dynamics [5, 6, 8, 18], structural mechanics [1, 3, 15, 22, 24], and electromagnetics [10, 9].

The reason for such extensive attention is mainly due to some important advantages of IGA methodology over more classical Finite Element Analysis (FEA). An example is the fact that IGA

numerical solutions can possess high regularity across mesh elements. This is an important feature, leading to a higher accuracy per degree-of-freedom (see [7, 17]), to improved spectrum properties of the discrete operators (see [20]), and the possibility of constructing discretizations able to preserve fundamental structures of the continuum differential operators (such as De Rham diagrams, see [9]).

However, within IGA approaches a remaining issue is the design of efficient quadrature rules taking advantage of high inter-element regularity. In fact, the technique adopted heretofore in the literature is to use Gauss quadrature on each element, a choice far from being optimal.

The aim of the present paper is to design an efficient quadrature strategy, in the sense that it should result in a considerable savings in terms of computational effort compared to classical Gauss rules, while maintaining the classical element-by-element assembly procedure.

The construction of quadrature rules for IGA was initially considered in [21]. The rule proposed therein is optimal because it exactly integrates B-spline basis functions with the minimum number of function evaluations; however, such an optimal quadrature rule is obtained as a solution of a *global, non-linear* and, in general, *ill-conditioned system* of equations, which is therefore difficult to solve for high polynomial degrees and numbers of elements. Moreover, such a quadrature rule *has to be recomputed when the number of elements changes*. As a consequence, in [21] the authors suggest utilizing the rule in a non-optimal way, considering the function regularity only at the level of small groups of elements (so-called macro-elements).

The present paper takes advantage of the translation-invariance of the basis functions defined in the domain interior, leading to a quadrature rule obtained solving a *local, non-linear system* of equations, which *does not have to be recomputed when the number of elements varies*. As a consequence, the new rule competes well with the optimal one proposed in [21] in terms of efficiency, but is much simpler to construct. However, special considerations needs to be given to elements on the boundary.

The rule is initially designed for the case of a uniform discretization of elements in the parametric domain, but is then extended to the case of geometrically refined meshes.

The paper is organized as follows. Section 2 describes some preliminaries on IGA and quadrature. Section 3 discusses one-dimensional B-splines, and presents the new quadrature rule, first for a periodic uniform knot vector and then for an open uniform knot vector, detailing the algorithm and discussing optimality. Section 4 exploits the new quadrature rule to numerically solve

boundary value problems, including one whose solution possesses sharp boundary layers. Section 5 gives some final comments.

2. Preliminaries on IGA and quadrature

For the sake of simplicity, the following presentation focuses on a two-dimensional setting, which can be easily converted to situations with a different dimensionality. Accordingly, introducing a parametric domain $\hat{\Omega} = [0, k] \times [0, k]$, the solution of classical engineering problems requires the calculation of integrals such as

$$\int_{\hat{\Omega}} R_{\mathbf{i}}(\boldsymbol{\xi}) R_{\mathbf{j}}(\boldsymbol{\xi}) \Phi(\boldsymbol{\xi}) d\boldsymbol{\xi}, \quad (2.1)$$

$$\int_{\hat{\Omega}} \nabla R_{\mathbf{i}}(\boldsymbol{\xi}) \nabla R_{\mathbf{j}}(\boldsymbol{\xi}) \Phi(\boldsymbol{\xi}) d\boldsymbol{\xi}, \quad (2.2)$$

$$\int_{\hat{\Omega}} \nabla R_{\mathbf{i}}(\boldsymbol{\xi}) R_{\mathbf{j}}(\boldsymbol{\xi}) \Phi(\boldsymbol{\xi}) d\boldsymbol{\xi}, \quad (2.3)$$

where: \mathbf{i} and \mathbf{j} are two-dimensional multi-indices; $R_{\mathbf{i}}$ and $R_{\mathbf{j}}$ are NURBS basis functions; Φ is a factor taking into account the coefficients of the investigated partial differential equation and the problem geometry, i.e., the Jacobian of the geometry map and, possibly, the derivatives of its inverse [13]. Typically, (2.1) emanates from a mass term, (2.2) from a stiffness term, while (2.3) corresponds to a linear advection term, classically encountered in fluid dynamics. Of course, one can consider also other terms, which could be included in the forthcoming discussion without any difficulty.

As commented in [21, Section 3.2], within isogeometric analysis it is a common practice to compute terms like (2.1)–(2.3) adopting quadrature rules able to exactly integrate the spline basis functions that generate the NURBS. Furthermore, in the case of tensor-product discretizations, the multi-dimensional quadrature rule is obtained from the tensor-product of suitable one-dimensional rules.

The one-dimensional integrals of interest are of the following kind

$$\begin{aligned} & \int_0^k \phi_{\mathbf{i}}(x) \phi_{\mathbf{j}}(x) dx, \\ & \int_0^k \phi'_{\mathbf{i}}(x) \phi'_{\mathbf{j}}(x) dx, \\ & \int_0^k \phi'_{\mathbf{i}}(x) \phi_{\mathbf{j}}(x) dx, \end{aligned} \quad (2.4)$$

where ϕ_i and ϕ_j belong to a proper space of univariate spline functions. Assuming the use of the approximation space S_r^p , i.e., the space of spline functions of degree p and regularity r , examining Equation (2.4), we may conclude that for the design of an exact quadrature rule the space of integrand functions to be considered is S_{r-1}^{2p} .

Considering as an example the interesting case of shape functions with maximum regularity, i.e., $\phi_i \in S_{p-1}^p$, we have:

$$\begin{aligned}\phi_i\phi_j &\in S_{p-1}^{2p}, \\ \phi_i'\phi_j' &\in S_{p-2}^{2p-2}, \\ \phi_i'\phi_j &\in S_{p-2}^{2p-1},\end{aligned}\tag{2.5}$$

and, therefore, S_{p-2}^{2p} is the space that contains all the integrands.

To generalize the discussion, in the following we indicate the space of the functions to be integrated as S_q^m , where m denotes the degree of the functions to be integrated and q denotes the corresponding regularity; clearly, the quantities m and q come from the original problem of interest (i.e., from Equations (2.4) and (2.5)), hence they should satisfy relation

$$m = 2p \quad , \quad q \leq p - 1,$$

from which it can also be derived

$$q \leq \left\lceil \frac{m}{2} \right\rceil - 1, \tag{2.6}$$

where $\lceil s \rceil$ is the smallest integer l such that $s \leq l$. Even though in this context $m = 2p$, we allow $m \in \mathbb{N}$ for the sake of generality.

3. Quadrature of univariate splines

Consistent with the previous discussion, we now aim to construct a quadrature rule able to exactly evaluate an integral in the form

$$\int_0^k \psi_i(x) dx$$

for the case of a spline function $\psi_i \in S_m^q$, where m and q are related by (2.6).

To this end we recall that, given a generic function f , an *n-point quadrature rule* is a choice of n ordered points and weights (x_i, w_i) such that

$$\int_a^b f(x) dx \simeq \sum_{i=1}^n w_i f(x_i).$$

A quadrature rule is said to be *exact* on the family of functions $\{f_j\}_{j=1,\dots,M}$ if

$$\int_a^b f_j(x) dx = \sum_{i=1}^n w_i f_j(x_i) \quad \forall j = 1, \dots, M. \quad (3.1)$$

Condition (3.1) represents M non-linear equations in the $2n$ unknowns (x_i, w_i) . Classically, exactness is required on polynomials up to a fixed degree; in particular, the n -point Gauss rule is the (only) n -point rule that is exact for polynomials up to degree $2n - 1$.

Recently, exactness on general families of functions has been also explored. For example, in [23, 12] a quadrature rule that integrates exactly M independent functions $\{f_j\}$ using $\left\lceil \frac{M}{2} \right\rceil$ points is introduced and named *Generalized Gaussian* with respect to the functions $\{f_j\}$.

With the previously addressed general consideration, to properly approach the problem of our interest, in the following we provide some details on one-dimensional B-splines (Section 3.1). We then approach the quadrature problem, for a periodic uniform knot vector (Section 3.2) and for an open uniform knot vector (Section 3.3), presenting also an algorithmic description (Section 3.4) and a discussion on the optimality (Section 3.5) for the newly proposed quadrature rule.

3.1. B-splines in one space dimension

As a one-dimensional parametric domain, referred to as a *patch*, we assume the interval $[0, k]$ with a uniform subdivision into unitary elements $[j - 1, j]$, where $j = 1, \dots, k$.

A spline function $f \in S_q^m$ is a polynomial of degree m in each element $[j - 1, j]$ with $f \in C^q([0, k])$. Accordingly, to determine a function $f \in S_q^m$, we need to assign $m + 1$ polynomial coefficients on each of the k elements with $q + 1$ continuity requirements on the $k - 1$ internal points; therefore, indicating by N the dimension of the space S_q^m , the following relation holds:

$$N = k(m + 1) - (k - 1)(q + 1) = k(m - q) + q + 1.$$

In general, $q \leq m - 1$ is allowed, even though in this paper we further restrict to condition (2.6). We also assume $q \geq -1$, where $q = -1$ refers to the discontinuous case, while $q = 0$ refers to the case of functions continuous on the whole domain $[0, k]$ and piecewise polynomial on each single element, i.e., the classical FEA approximation.

Following a standard procedure in the B-spline literature [25], to construct the basis functions we define a *knot vector* in the form

$$\{\xi_1, \xi_2, \dots, \xi_{N+m+1}\}$$

In particular, as a first case we consider an *open* uniform knot vector Ξ , defined as

$$\Xi = \left\{ \underbrace{0, \dots, 0}_{m+1 \text{ times}}, \underbrace{1, \dots, 1}_{m-q \text{ times}}, \dots, \underbrace{k-1, \dots, k-1}_{m-q \text{ times}}, \underbrace{k, \dots, k}_{m+1 \text{ times}} \right\} \quad (3.2)$$

where the first and last knots, i.e., 0 and k , have multiplicity $(m+1)$, and the other knots have multiplicity $(m-q)$. Starting from Ξ , we can construct the basis functions $\{\psi_j\}_{j=1, \dots, N}$ for the space S_q^m , using the following recursive formula

$$\psi_j^\ell(x) = \frac{x - \xi_j}{\xi_{j+\ell} - \xi_j} \psi_j^{\ell-1}(x) + \frac{\xi_{j+\ell+1} - x}{\xi_{j+\ell+1} - \xi_{j+1}} \psi_{j+1}^{\ell-1}(x), \quad \ell = 1, \dots, m, \quad (3.3)$$

with the initial condition

$$\psi_j^0(x) = \begin{cases} 1 & \text{if } \xi_j \leq x < \xi_{j+1} \\ 0 & \text{otherwise} \end{cases}$$

and setting

$$\psi_j(x) = \psi_j^m(x).$$

We recall the convention that, when a denominator is zero in (3.3), the corresponding quotient is set to zero.

Similarly, we can introduce a *periodic* uniform knot vector $\tilde{\Xi}$, defined as

$$\tilde{\Xi} = \left\{ \underbrace{0, \dots, 0}_{m-q \text{ times}}, \underbrace{1, \dots, 1}_{m-q \text{ times}}, \dots, \underbrace{k-1, \dots, k-1}_{m-q \text{ times}}, \underbrace{k, \dots, k}_{m-q \text{ times}} \right\} \quad (3.4)$$

and, adopting the recursive scheme indicated in (3.3), we can construct the basis functions associated to $\tilde{\Xi}$ and spanning a space denoted as \tilde{S}_q^m . We observe that $\tilde{S}_q^m \subset S_q^m$ and, in particular, that $\tilde{S}_q^m = \text{span} \{\psi_j\}_{j=q+2, \dots, N-q-1}$.

We recall that with this construction each basis function is non-negative and

$$\text{supp } \psi_j = [\xi_j, \xi_{j+m+1}];$$

therefore, since for the specific cases of interest we have an $m-q$ multiplicity of internal knots (e.g., Equations (3.2) and (3.4)) as well as restriction (2.6) on m and q , each B-spline basis function ψ_j can have support in at most two elements.

Accordingly, we introduce a new notation, to distinguish between basis functions having support only in one element and basis functions having support on two elements. In particular, we indicate with the superscript (i) the basis functions that have support included in the element $[i-1, i]$ and with the superscript $(i, i+1)$ those with support in $[i-1, i+1]$.

Moreover, we observe that the basis functions $\psi_j \in S_q^m$ with support only on one element can be further distinguished into a set of *boundary functions*, in the following also indicated with a superposed bar, which are present only in the first and the last element, as a consequence of the fact that the first and the last knot have multiplicity $m + 1$, and a set of *bubble functions*, which are instead present in all the elements, i.e., both in the boundary as well as in the internal ones. Finally, all the functions with support on two elements are referred to as *transmission functions*.

The whole set of basis functions for the space S_q^m can be rearranged distinguishing between three groups of functions:

- $2(q + 1)$ boundary functions $\bar{\psi}_j^{(i)}$, $1 \leq j \leq q + 1, i = 1, k$;
- $k(m - 2q - 1)$ bubble functions $\psi_j^{(i)}$, $1 \leq j \leq m - 2q - 1, 1 \leq i \leq k$;
- $(k - 1)(q + 1)$ transmission functions $\psi_j^{(i, i+1)}$, $1 \leq j \leq q + 1, 1 \leq i \leq k - 1$.

As an example, for the case $m = 10, k = 3$ with $q = 3$, Figure 1 reports all the basis functions generated from the open uniform knot vector, while Figure 2 reports the same basis functions, distinguishing between boundary, bubble and transmission functions. We observe that

- the $q + 1$ boundary functions on the first element are related to the $q + 1$ boundary functions on the last element by the following: $\bar{\psi}_j^{(1)}(x) = \bar{\psi}_{q+2-j}^{(k)}(k - x)$ (we will say that they are *specular*);
- the bubble functions are such that $\forall i_1, i_2 \in \{1, \dots, k\}$ the following translation property holds: $\psi_j^{(i_1)}(x) = \psi_j^{(i_2)}(x - (i_1 - i_2))$;
- the transmission functions are such that $\forall i_1, i_2 \in \{1, \dots, k - 1\}$ the following translation property holds: $\psi_j^{(i_1, i_1+1)}(x) = \psi_j^{(i_2, i_2+1)}(x - (i_1 - i_2))$.

Recalling that $\tilde{S}_q^m \subset S_q^m$, we observe that the space \tilde{S}_q^m is spanned by:

- $k(m - 2q - 1)$ bubble functions $\psi_j^{(i)}$, $1 \leq j \leq m - 2q - 1, 1 \leq i \leq k$;
- $(k - 1)(q + 1)$ transmission functions $\psi_j^{(i, i+1)}$, $1 \leq j \leq q + 1, 1 \leq i \leq k - 1$.

At this stage it is fundamental to observe that all functions in \tilde{S}_q^m are translation invariant, and this property will be used in the construction of an optimal rule for exact quadrature in Section 3.2. Since \tilde{S}_q^m and S_q^m differ only by the presence of the boundary functions in S_q^m , in Section

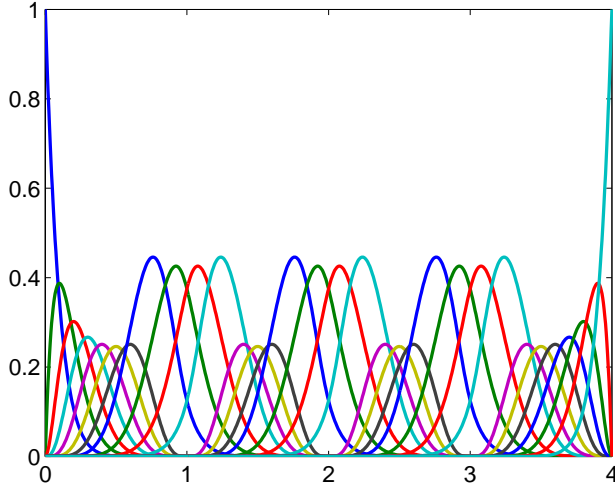


Figure 1: Basis functions generated by the open uniform knot vectors for the case $m = 10, k = 4, q = 3$.

3.3 we will reach our final goal of developing an exact quadrature for S_q^m , enriching the rule for \tilde{S}_q^m in order to integrate the additional boundary functions.

3.2. Quadrature on a periodic uniform knot vector

The first problem we want to address is the construction of an exact quadrature rule for $\psi_j \in \tilde{S}_q^m$. As we have seen in the previous section, these functions can be grouped in bubble and transition functions that are repeated up to translation on each element or couple of elements, respectively. Because of the translation properties of the functions to be integrated, we also assume that the quadrature rule is the same in all elements. That is, for $i \in \{1, \dots, k\}$ and $l = 1, \dots, n^I$, if $x_l^{I,i}$ and $w_l^{I,i}$ are the quadrature points in $[i-1, i]$ and quadrature weights, respectively, we take

$$x_l^{I,i} = x_l^I + (i-1), \text{ and } w_l^{I,i} = w_l^I,$$

with $x_l^I \in [0, 1]$. The number of quadrature points per element is denoted by n^I , and will be determined later. Then, the problem of the exact integration of the bubble functions $\psi_j^{(i)}$

$$\sum_{l=1}^{n^I} w_l^{I,i} \psi_j^{(i)}(x_l^{I,i}) = \int_{i-1}^i \psi_j^{(i)}(x) dx, \quad 1 \leq j \leq m - 2q - 1,$$

and exact integration of the transition functions $\psi_j^{(i,i+1)}$ (for $i \in \{1, \dots, k-1\}$)

$$\sum_{l=1}^{n^I} w_l^{I,i} \psi_j^{(i,i+1)}(x_l^{I,i}) + \sum_{l=1}^{n^I} w_l^{I,i+1} \psi_j^{(i,i+1)}(x_l^{I,i+1}) = \int_{i-1}^{i+1} \psi_j^{(i,i+1)}(x) dx, \quad 1 \leq j \leq q + 1$$

can be summarized as follows

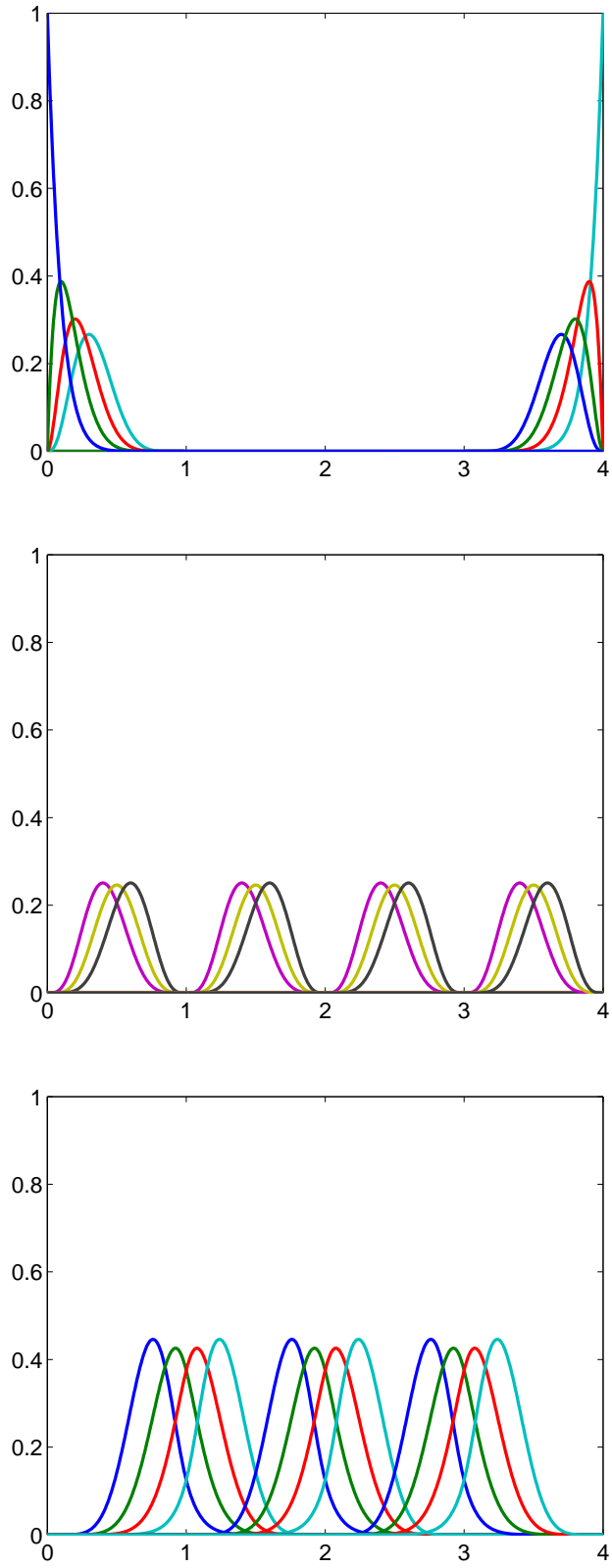


Figure 2: Basis functions generated by the uniform open knot vector for the case $m = 10, k = 4, q = 3$, distinguishing between boundary functions, bubble functions and transmission functions, respectively.

Problem 3.1 (Quadrature for Periodic Problem). *For a given $i \in \{1, \dots, k-1\}$, find quadrature points $x_l^I \in [0, 1]$, and weights $w_l^I > 0$, $l = 1, \dots, n^I$ such that*

$$\left\{ \begin{array}{l} \sum_{l=1}^{n^I} w_l^I \psi_j^{(i)}(x_l^I + (i-1)) = \int_{i-1}^i \psi_j^{(i)}(x) dx, \quad 1 \leq j \leq m-2q-1 \\ \sum_{l=1}^{n^I} w_l^I \left[\psi_j^{(i,i+1)}(x_l^I + (i-1)) + \psi_j^{(i,i+1)}(x_l^I + i) \right] \\ = \int_{i-1}^{i+1} \psi_j^{(i,i+1)}(x) dx \quad 1 \leq j \leq q+1. \end{array} \right. \quad (3.5)$$

□

Since (3.5) is a system of $m-q$ equations, we look for $n^I = \left\lceil \frac{(m-q)}{2} \right\rceil$ quadrature points and weights.

In particular, for the case $(m-q)$ even, we have a square non-linear system of equations and, as shown in the numerical simulations in Section 4, this leads to two possible solutions, specular in each element. This is not in contradiction with the uniqueness result for Generalized Gauss quadrature rules as available in [12], since the functions that we are integrating do not satisfy the hypothesis of this result, in particular they are not a Chebychev System. On the other hand, for the case $(m-q)$ odd, we have several admissible solutions. Among these, there is one that is symmetric in the element and our choice is to select exactly this one. To this purpose, we complement (3.5) with the condition $x_1^I + x_{n^I}^I = 1/2$.

We introduce now the functions $\{\eta_j\}_{j=1, \dots, m-q}$ such that

$$\left\{ \begin{array}{l} \eta_j(x) = \psi_j^{(i)}(x+i) \quad j = 1, \dots, m-2q-1 \\ \eta_j(x) = \psi_h^{(i,i+1)}(x+i) + \psi_h^{(i,i+1)}(x+i+1) \quad j = m-2q, \dots, m-q \\ \text{and } h = j - m + 2q + 1, \end{array} \right. \quad (3.6)$$

for all $x \in [0, 1]$. The functions η_j are $(m-q)$ functions, independent of i , with support on $[0, 1]$ such that:

$$\begin{aligned} \int_0^1 \eta_j(x) dx &= \int_{i-1}^i \psi_j^{(i)}(x) dx \quad j = 1, \dots, m-2q-1 \\ \int_0^1 \eta_j(x) dx &= \int_{i-1}^{i+1} \psi_h^{(i,i+1)}(x) dx \quad j = m-2q, \dots, m-q; \quad h = j - m + 2q + 1 \end{aligned}$$

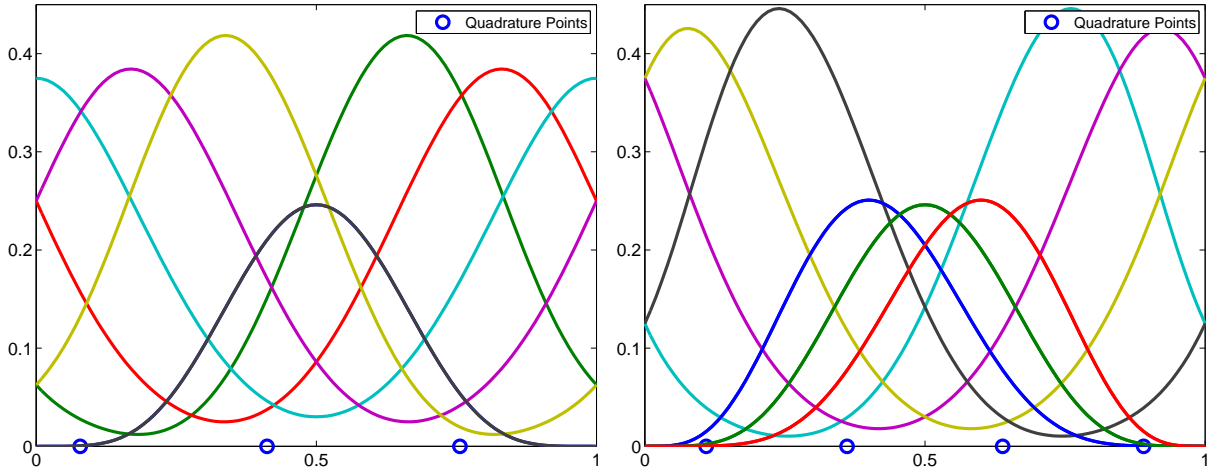


Figure 3: Functions to be exactly integrated by the quadrature rule in Problem 3.2, namely functions $\eta_j(x)$ of Equations (3.6). A choice of the resulting quadrature points is plotted on the x axis. On the left is the case with $m = 10, k = 3, q = 4$, on the right is the case with $m = 10, k = 3, q = 3$.

Figure 3 shows for two choices of m, k and q the functions $\eta_j(x)$ and the resulting quadrature points. Setting

$$\mathcal{M}_j \equiv \int_0^1 \eta_j(x) dx,$$

we can rewrite Problem 3.1 in an equivalent form as follows

Problem 3.2. Find $x_l^I \in [0, 1]$ and $w_l^I > 0$, $l = 1, \dots, n^I$ such that

$$\sum_{l=1}^{n^I} w_l^I \eta_j(x_l^I) = \mathcal{M}_j.$$

□

This is the only non-linear problem that needs to be solved in our final algorithm. We stress that the dimension of this non-linear problem only depends on the degree m and regularity q and it is independent of k , i.e., it is independent of the number of elements introduced in the discretization.

However, when m is large, Problem 3.2 can be ill-conditioned, and for this reason we deal with it following the approach proposed in [12]. Assuming for simplicity $(m - q)$ to be even¹, we

¹Remember that in the case $(m - q)$ odd we consider one new equation imposing symmetry and recover the square dimension. This modifies the functional \mathbb{G} described below, although the Jacobian can be calculated also in this case.

introduce the following functional \mathbb{G} defined as

$$\mathbb{G} : \mathbb{R}^{2n^I} \rightarrow \mathbb{R}^{2n^I}, \quad 2n^I = m - q$$

where

$$\mathbb{G}_j(x_1, \dots, x_{n^I}, w_1, \dots, w_{n^I}) = \sum_{l=1}^{n^I} w_l \eta_j(x_l) - \mathcal{M}_j.$$

With this notation, the solution of Problem 3.2 is a zero of the above functional:

$$\mathbb{G}(\mathbf{x}^I, \mathbf{w}^I) = \mathbf{0}.$$

Now, the Jacobian of functional \mathbb{G} can be easily constructed explicitly since the derivatives of the basis functions are known, in fact:

$$\frac{\partial \mathbb{G}_j}{\partial x_i} = w_i \eta_j'(x_i), \quad \frac{\partial \mathbb{G}_j}{\partial w_i} = \eta_j(x_i)$$

Thus, Newton iterations can be constructed. It is important to observe that the choice of the starting point is crucial to obtain convergence, due to the possible ill-conditioning of the Jacobian matrix. As proposed in [12], we use a continuation algorithm to obtain better conditioned sub-problems. Therefore, we are led to solve the following:

Problem 3.3. Fix $(x_1^{(0)}, \dots, x_{n^I}^{(0)}, w_1^{(0)}, \dots, w_{n^I}^{(0)})$ and a sequence of increasing $\alpha_{it} \in (0, 1]$, $it = 1, \dots, n_{it}$, with $\alpha_{n_{it}} = 1$.

For all $it = 1, \dots, n_{it}$, find $(x_1^{(it)}, \dots, x_{n^I}^{(it)}, w_1^{(it)}, \dots, w_{n^I}^{(it)})$ s.t. $\mathbb{G}^{(it)}(x_1^{(it)}, \dots, x_{n^I}^{(it)}, w_1^{(it)}, \dots, w_{n^I}^{(it)}) = \mathbf{0}$, where we define:

$$\begin{aligned} & \mathbb{G}_j^{(it)}(x_1, \dots, x_{n^I}, w_1, \dots, w_{n^I}) \\ & \equiv \sum_{l=1}^{n^I} w_l \eta_j(x_l) - \alpha_{it} \left[\int_0^1 \eta_j(x) dx \right] - (1 - \alpha_{it}) \left[\sum_{l=1}^{n^I} w_l^{(it-1)} \eta_j(x_l^{(it-1)}) \right]. \end{aligned}$$

□

We propose to use as initial choice $(x_1^{(0)}, \dots, x_{n^I}^{(0)}, w_1^{(0)}, \dots, w_{n^I}^{(0)})$ the Gauss nodes and equal weights, and a vector of parameters α_{it} fitted near zero.

Summarizing, the solution of Problem 3.1 is given by $x_l^I = x_l^{(n_{it})}$, and $w_l^{I,i} = w_l^{(n_{it})}$, for $l = 1, \dots, n^I = (m - q)/2$.

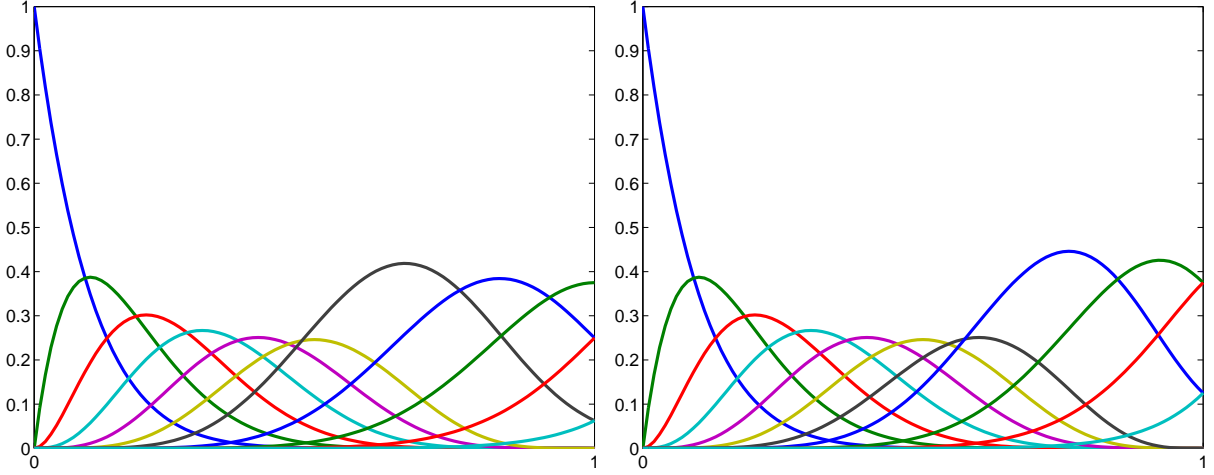


Figure 4: Functions to be integrated by the boundary quadrature rule, namely functions $\bar{\psi}_j^{(1)}(x)$, $\psi_j^{(1)}(x)$ and $\psi_j^{(1,2)}(x)$ truncated to the first element. Note that the rule has to give the inexact result for the latter, see Equation (3.7). On the left is the case with $m = 10, k = 3, q = 4$, on the right is the case with $m = 10, k = 3, q = 3$.

3.3. Quadrature on an open uniform knot vector

As commented in Section 3.1, the spline space S_q^m generated by the open uniform knot vector is larger than the space \tilde{S}_q^m considered in the previous section, since it contains also the boundary functions $\bar{\psi}_1^{(1)}, \dots, \bar{\psi}_{q+1}^{(1)}$ and $\bar{\psi}_1^{(k)}, \dots, \bar{\psi}_{q+1}^{(k)}$. Then, the quadrature rule of Section 3.2 needs to be modified properly at the boundary.

For exposition purposes, we focus on the left boundary; thus, we have to construct a quadrature rule for the basis functions whose support contains $[0, 1]$. Following the notation introduced in Section 3.1, such basis functions coincide with the first $m + 1$ basis functions of the spline space S_q^m , that is

$$\{\psi_i\}_{i=1, \dots, m+1} \equiv \{\bar{\psi}_1^{(1)}, \dots, \bar{\psi}_{q+1}^{(1)}, \psi_1^{(1)}, \dots, \psi_{m-2q-1}^{(1)}, \psi_1^{(1,2)}, \dots, \psi_{q+1}^{(1,2)}\}.$$

and these functions are plotted in Figure 6 for two choices of m, k and q .

We note that that the set $\{\psi_i|_{[0,1]}\}_{i=1, \dots, m+1}$ is a basis for the polynomials of degree m on the first element $[0, 1]$.

Our aim is to solve the following:

Problem 3.4 (Boundary Quadrature). *Find n^B quadrature points $x_l^B \in [0, 1]$, and weights w_l^B , $l = 1, \dots, n^B$ such that:*

$$\sum_{l=1}^{n^B} w_l^B \psi_i(x_l^B) = \int_0^1 \psi_i(x) dx - \sum_{l=1}^{n^I} w_l^{I,2} \psi_i(x_l^{I,2}), \quad i = 1, \dots, m + 1, \quad (3.7)$$

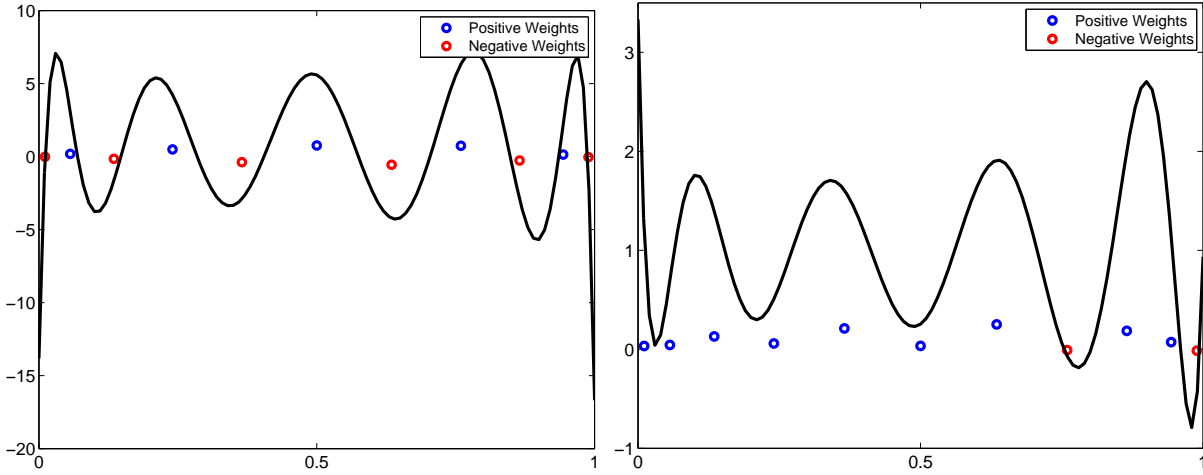


Figure 5: The resulting quadrature on the boundary: the function $g(x)$ defined in (3.8) and the quadrature rule in the case of $m + 1 = 11$ Gauss nodes. On the left in the case $m = 10; k = 3; q = 4$ and on the right in the case $m = 10; k = 3; q = 3$.

where $x_l^{I,2}, w_l^{I,2}$ are the quadrature points and weights from Problem (3.1). □

In order to represent the right hand side of (3.7) in a more convenient way, we introduce a function $g(x)$ such that

$$\int_0^1 \psi_i(x)g(x)dx = \int_0^2 \psi_i(x)dx - \sum_{l=1}^{n^I} w_l^{I,2}\psi_i(x_l^{I,2}). \quad (3.8)$$

Function $g(x)$ can be chosen as an m -degree polynomial and can be easily computed, see Section 3.4. Then we have the following weighted quadrature problem equivalent to Problem 3.4.

Problem 3.5. Find n^B quadrature points $x_l^g \in [0, 1]$, and weights $w_l^g, l = 1, \dots, n^B$ such that:

$$\sum_{l=1}^{n^B} w_l^B \psi_j(x_l^B) = \int_0^1 \psi_j(x)g(x)dx \quad \forall j = 1, \dots, m + 1. \quad (3.9)$$

□

Solving Problem 3.5 is equivalent to finding a quadrature rule with respect to the weighted measure $g(x)dx$, requiring exactness for polynomials of degree m on $[0, 1]$. Since $g(x)$ has in general oscillating sign, the existence of a quadrature rule with $(m + 1)/2$ points is not guaranteed in this context. However, we can use an $(m + 1)$ -nodes standard Gauss rule (x_l^G, w_l^G) : it integrates exactly the polynomials of degree $2m + 1$, and in particular, all the products $\psi_j(x)g(x)$. Thus we have:

$$\int_0^1 \psi_j(x)g(x)dx = \sum_{l=1}^{m+1} w_l^G \psi_j(x_l^G)g(x_l^G). \quad (3.10)$$

Problem 3.5 is then solved for $n^B = m + 1$ by setting $w_l^B = w_l^G g(x_l^G)$ and $x_l^B = x_l^G$.

In Figure 5 the quadrature rule is plotted. Notice that some of the final weights are negative. Related stability issues are discussed in Remark 3.1.

The advantage of this procedure is that $g(x)$ can be accurately and easily computed. For this purpose, we introduce an auxiliary basis $\{\zeta_i\}$ for the space of polynomials of degree m on $[0, 1]$. Choosing $\zeta_j = \psi_j$ our algorithm (see Section 3.4) works up to machine precision for $m \leq 16$. If we choose instead $\zeta_j(x)$ as the Legendre polynomials we can go up to degree $m = 32$.

To summarize, suppose to have solved Problem 3.2 and Problem 3.4 (for the left boundary $(x_l^{LB}, w_l^{LB}) = (x_l^B, w_l^B)$ and for the right boundary (x_l^{RB}, w_l^{RB}) in the analogous way), then the quadrature rule for exact integration of all $f \in S_q^m$ is

$$\int_0^k f(x) dx \simeq \sum_{l=1}^{n^B} w_l^{LB} f(x_l^{LB}) + \sum_{i=1}^{k-2} \left(\sum_{l=1}^{n^I} w_l^I f(x_l^I + i) \right) + \sum_{l=1}^{n^B} w_l^{RB} f(x_l^{RB}).$$

We remark that if $m - q$ is odd, the two boundary problems are specular and (x_l^{RB}, w_l^{RB}) are immediately obtained from (x_l^{LB}, w_l^{LB}) .

Remark 3.1. *Stability of a quadrature rule, and its convergence on C^0 integrand functions as the number of quadrature points increases, is guaranteed when the sum of the weight absolute values is uniformly bounded, see for example [11]. In the case of (3.3), we easily have that*

$$\sum_{l=1}^{n^I} |w_l^I| = 1,$$

since internal weights w_l^I are positive (recall Problem 3.1). Furthermore, in all our numerical tests, up to $m = 32$, we have always observed that $\sum_{l=1}^{n^B} |w_l^{LB}|$ is bounded, therefore, despite that some quadrature weights on the boundary elements may be negative, the stability of the overall procedure is guaranteed.

Remark 3.2. *One can also consider alternative procedures to avoid negative weights. As in Problem 3.2, one can try to numerically compute the quadrature points x_l^B and weights w_l^B in Problem 3.5, constraining the w_l^B to be positive. Existence of the solution is not guaranteed but our experience shows that a solution can be found with, e.g., $n^B = m + 1$, as in (3.10).*

3.4. Quadrature algorithm

A pseudo-code for the numerical evaluation of the quadrature points and weights is proposed in this section, again for simplicity in the case of $m - q$ even. The output is the nodes and weights

for internal, left boundary and right boundary. All the three sets of nodes are calculated in $[0, 1]$, thus, once computed, they have to be properly shifted in the patch.

Input: $m =$ spline degree; $q =$ spline regularity;

Set $n^I = (m - q)/2$, $n^B = m + 1$;

{Computation of the quadrature rule on internal elements}

Set α be a vector of n_{it} ordered real numbers s.t. $\alpha(i) > 0$, $\alpha(n_{it}) = 1$.

Calculate \mathcal{M}_j , exact integrals of functions $\eta_j(x)$ defined in (3.6);

Initialize $x_j^{(0)}$, $w_j^{(0)}$;

for $i = 1, \dots, n_{it}$ **do** {see Problem 3.3}

 Compute $w_l^{(i)}$, $x_l^{(i)}$ such that

$$\begin{cases} w_l^{(i)} > 0, x_l^{(i)} \in [0, 1], \forall l = 1, \dots, n^I \text{ and} \\ \sum_{l=1}^{n^I} w_l^{(i)} \eta_j(x_l^{(i)}) - \alpha(i) \mathcal{M}_j - (1 - \alpha(i)) \left[\sum_{l=1}^{n^I} w_l^{(i-1)} \eta_j(x_l^{(i-1)}) \right] = 0. \end{cases} \quad (3.11)$$

end for

Set $(x_l^I, w_l^I) = (x_l^{(n_{it})}, w_l^{(n_{it})})$.

{Computation of the quadrature rule on the left boundary element}.

Calculate $A \equiv (a_{ij})_{i,j=1,\dots,m+1}$, $a_{ij} = \int_0^1 \psi_i(x) \zeta_j(x) dx$;

Calculate $\lambda_i \equiv \int_0^2 \psi_i(x) dx - \sum_{l=1}^{n^I} w_l^I \psi_i(x_l^I + 1)$;

Solve the linear problem $A\beta = \lambda$ and set $g(x) = \sum_{j=1}^{m+1} \beta_j \zeta_j(x)$;

Calculate a n^B -points quadrature rule $(x_l^{LB}, w_l^{LB}) = (x_l^B, w_l^B)$ of degree of exactness m for the weighted measure $g(x)dx$. {e.g., use (3.10)}.

{Computation of the quadrature rule on the right boundary element}.

Calculate in a similar way (x_l^{RB}, w_l^{RB}) .

return Internal n^I -points quadrature rule (x_l^I, w_l^I) and two boundary n^B -points quadrature rules (x_l^{LB}, w_l^{LB}) , (x_l^{RB}, w_l^{RB}) .

In all our tests system (3.11) is solved by the MATLAB Optimization Toolbox *fsolve* routine (see [26]), setting a machine-precision tolerance on the residual norm. The complete MATLAB

implementation for the calculation of the interior and boundary quadrature is available in the `Contributions` section at `geopdes.sourceforge.net`.

Below, we also report the pseudo code for the alternative calculation of the quadrature rule at the boundary, with enforcement of positivity of the weights, as described in Remark 3.2.

Set n^B , e.g., $n^B = m + 1$;
 {Alternative computation of the quadrature rule on the left boundary element}
 Calculate $\lambda_i \equiv \int_0^2 \psi_i(x) dx - \sum_{l=1}^{n^B} w_l^I \psi_i(x_l^I + 1)$;
 Compute w_l, x_l such that

$$\begin{cases} w_l > 0, x_l \in [0, 1], & \forall l = 1, \dots, n^B \text{ and} \\ \sum_{l=1}^{n^B} w_l \psi_i(x_l) - \lambda_i = 0, & \forall i = 1, \dots, m + 1 \end{cases} \quad (3.12)$$

Set $(x_l^{LB}, w_l^{LB}) = (x_l, w_l)$.

3.5. Optimality of the new quadrature rule

In the previous sections we have proposed a new quadrature rule, which can be computed in an efficient and stable manner. We now want to discuss the optimality of the proposed quadrature rule.

We observe the following.

- In each space dimension, the proposed rule uses $(k - 2) \left\lceil \frac{m - q}{2} \right\rceil + 2(m + 1)$ quadrature points, with $m = 2p$ and $q = r - 2$, when NURBS of degree p and regularity r are selected for the IGA of an elliptic second order problem.
- The optimal quadrature rule proposed in [21] would require $\left\lceil k \frac{m - q}{2} + \frac{q + 1}{2} \right\rceil$ quadrature points in each dimension.
- Element-wise Gauss quadrature needs $k \left\lceil \frac{m + 1}{2} \right\rceil$ points per dimension instead.

According to these considerations, in Figure 6 we plot the number of quadrature points (i.e., the computational cost) for the three different quadrature rules reported above in the case of a uniform three-dimensional mesh of $k \times k \times k$ elements. The figure shows that the quadrature rule proposed in this paper has approximately the same number of quadrature points as the optimal one from

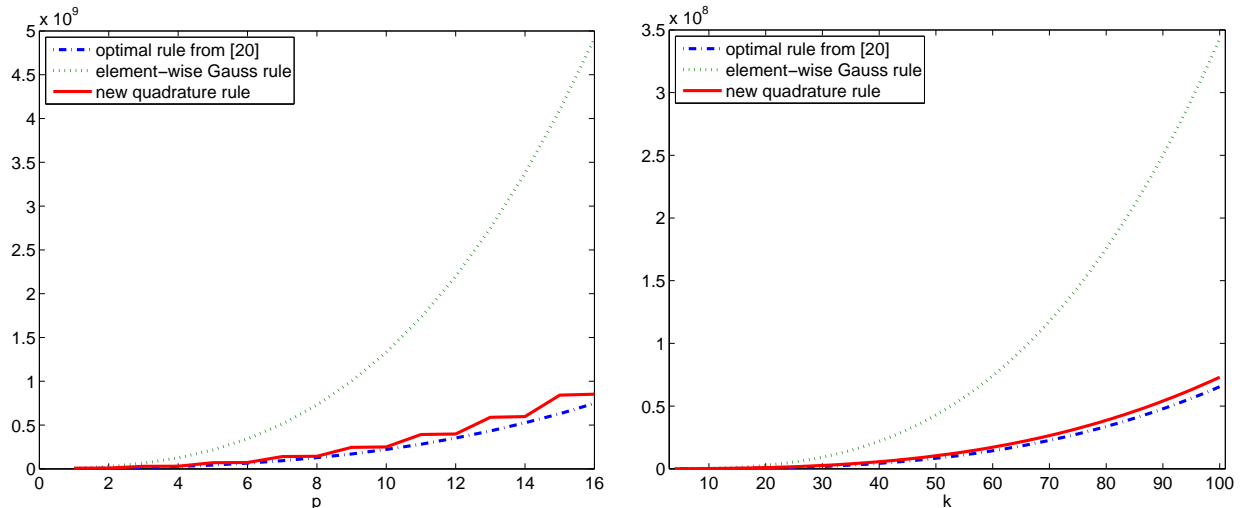


Figure 6: Comparison of the number of quadrature points needed for various quadrature rules on a $(k \times k \times k)$ -element three-dimensional mesh. On the left: $p = 1, \dots, 16$ ($m = 2p$), $q = p - 2$, and $k = 4, \dots, 100$, on the right: $p = 6$ ($m = 12$), $q = p - 2 = 4$, and $k = 4, \dots, 100$.

[21], which is approximately $1/8$ the number of quadrature points of the element-wise Gauss rule, for large k and p .

However, we recall that the optimal quadrature rule from [21] is in practice impossible to obtained for the cases considered in Figure 3.5 (i.e. p up to 16 and k up to 100), while the computation of quadrature points and weights for the new rule is straightforward with the algorithm discussed in Section 3.4.

4. Applications

We now present some applications of the proposed new quadrature rule. In particular, we prove its efficiency versus the element-wise Gauss quadrature rule, for boundary value problems in two-dimensions solved with a standard IGA formulation (see [13] for details). We remark that 2D (and 3D) integration rules are simply constructed as tensor products of 1D rules. We moreover discuss how to solve examples where some types of non-uniform meshes are considered. In particular, we show the behavior of the new rules on an example where a non-uniform, anisotropically graded mesh is used to capture a solution exhibiting thin layers.

4.1. Numerical solution of a Poisson problem on a quarter of an annulus

As a first example, a problem involving a non-trivial geometry that can be exactly represented by NURBS is considered. With this aim, we focus on a Poisson problem defined on a quarter of

an annulus Ω (see Figure 7) with an internal radius $R_1 = 1$ and an external radius $R_2 = 4$, and we solve the model problem:

$$\begin{cases} -\Delta u = f, & \forall x \in \Omega, \\ u|_{\partial\Omega} = 0, \end{cases} \quad (4.1)$$

with

$$\begin{aligned} f = & (2x^4 - 50x^2 - 50y^2 + 2y^4 + 4x^2y^2 + 100) \sin(x) \sin(y) + \\ & + (68x - 8x^3 - 8xy^2) \cos(x) \sin(y) + (68y - 8y^3 - 8yx^2) \cos(y) \sin(x), \end{aligned}$$

such that the exact solution is

$$u = (x^2 + y^2 - 1)(x^2 + y^2 - 16) \sin(x) \sin(y).$$

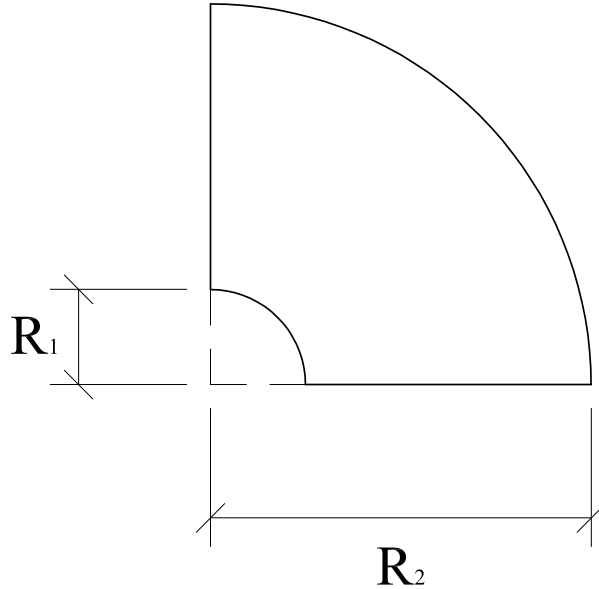


Figure 7: Poisson problem on a quarter of an annulus: geometry of the domain Ω .

We find an approximation of the solution by a standard IGA Galerkin formulation, using for integration the proposed new quadrature rules, as well as, for comparison reasons, a standard element-wise Gauss quadrature. The problem is solved for basis function degrees $p = q = 2, \dots, 5$ in both parametric directions (and maximum inter-element regularity), using control nets consisting of 25×25 up to 100×100 control points. In Figure 8, we show the convergence curves for the L^2 -norm of the relative error with respect to the exact solution. The theoretically expected rates

of convergence (i.e., $p + 1$) are obtained. In the same Figure, we also report the error computed with respect to the numerical solution obtained using element-wise Gauss quadrature. It can be seen that this error is always negligible with respect to the approximation error (a saturation is observed for high orders, when this error is in the range of machine-precision).

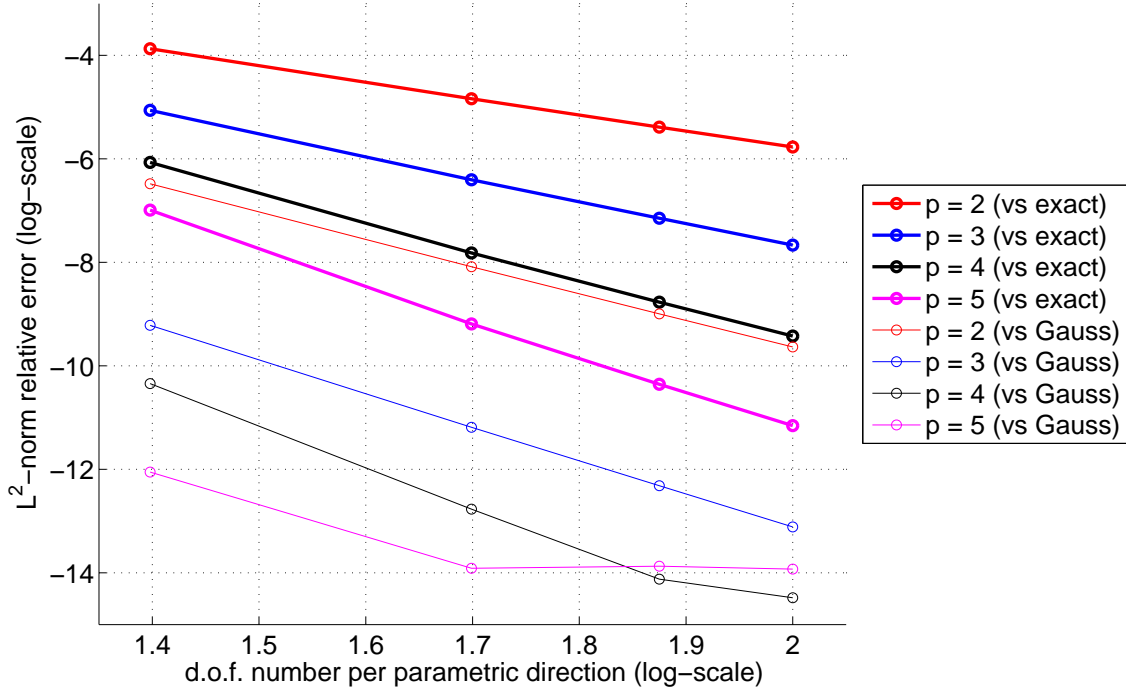


Figure 8: Poisson problem on a quarter of an annulus: convergence curves for the L^2 -norm of the relative error ($p = q = 2, \dots, 5$), using for integration the proposed new quadrature rules; errors are computed both with respect to the exact solution (thick curves) and to the numerical solution obtained using element-wise Gauss quadrature (thin curves).

In Figure 9 we report the total number of points used for integration by the two quadrature strategies. In particular, on the top, we show the number of quadrature points as a function of the number of control points for a fixed basis function degree $p = q = 4$ (and maximum inter-element regularity) in both parametric directions, while, on the bottom, we show the number of quadrature points as a function of the basis function degrees $p = q$ (always considering maximum regularity) for a fixed 100×100 control net. The advantage of the new rules is clear, in particular for high degrees (implying high inter-element regularity) and when the number of control points is not too low, that is, when the number of boundary elements (i.e., the number of elements where the rules are not optimal) is not large with respect to the number of internal elements.

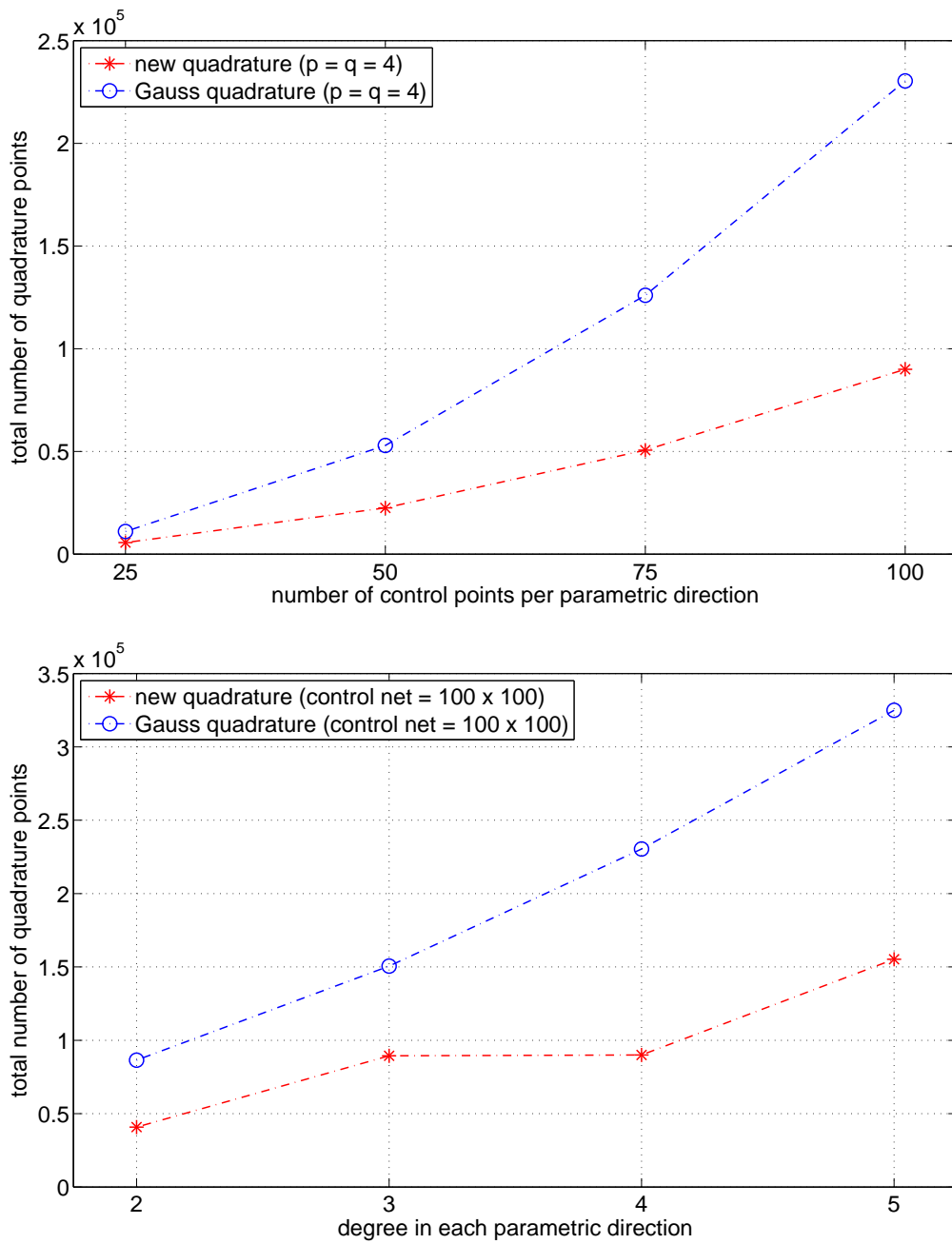


Figure 9: Poisson problem on a quarter of an annulus: number of quadrature points as a function of the number of control points for a fixed basis function degree $p = q = 4$ in both parametric directions (top); number of quadrature points as a function of the basis function degrees $p = q$ for a fixed 100×100 control net (bottom).

Finally, in Figure 10, we show the distribution of the points required by the two quadrature strategies in the case $p = q = 4$ when a 25×25 control net is adopted. The advantage of using the new rules is clear (5625 points versus the 11025 needed by Gauss quadrature), despite this case not being a very fine mesh (where, as seen above, such an advantage would be amplified).

4.2. Extension to non-uniform meshes

The theoretical part of the present paper focuses only on the construction of efficient quadrature rules for the case of uniform knot vectors. In this section, we sketch how to extend the proposed new quadrature rules to some particular, but useful, cases of non-uniform knot vectors. We however remark that, despite the fact that many of the typical cases of mesh refinement in IGA can be covered, as discussed in the following, a solution for more general non-uniform situations is not within the scope of this work.

4.2.1. Geometrically graded mesh

The problem of the extension of the proposed quadrature formula to non-uniform knot vectors is made difficult by the issue of the proper integration of transmission functions, which relies strongly on their translation-invariant property. The removal of the hypothesis of knot uniformity implies that, in general, such a translation-invariant property no longer holds. However, since all the functions to be exactly integrated on interior elements are supported over only two elements, a way to simply construct the new quadrature rules for a non-uniform knot vector is to constrain the ratio between the lengths of two consecutive knot spans to be fixed (i.e., a “geometrically graded” knot vector is considered). In this case, when considering pairs of consecutive elements, it is clear that transmission functions always have the same structure and, as a consequence, the previously described procedure for computing quadrature points and weights can be simply extended to this situation.

This is indeed an interesting case from the point of view of applications, since geometrically graded meshes are among the most used categories of non-uniform meshes and are, in particular, important when solution layers have to be captured (see, e.g., the example in the next section).

4.2.2. Quadrature multi-patch

We define *quadrature multi-patch* as the case of a mesh made of “sub-patches” where a different (but unique within each single sub-patch) quadrature rule is used. The sub-patches are

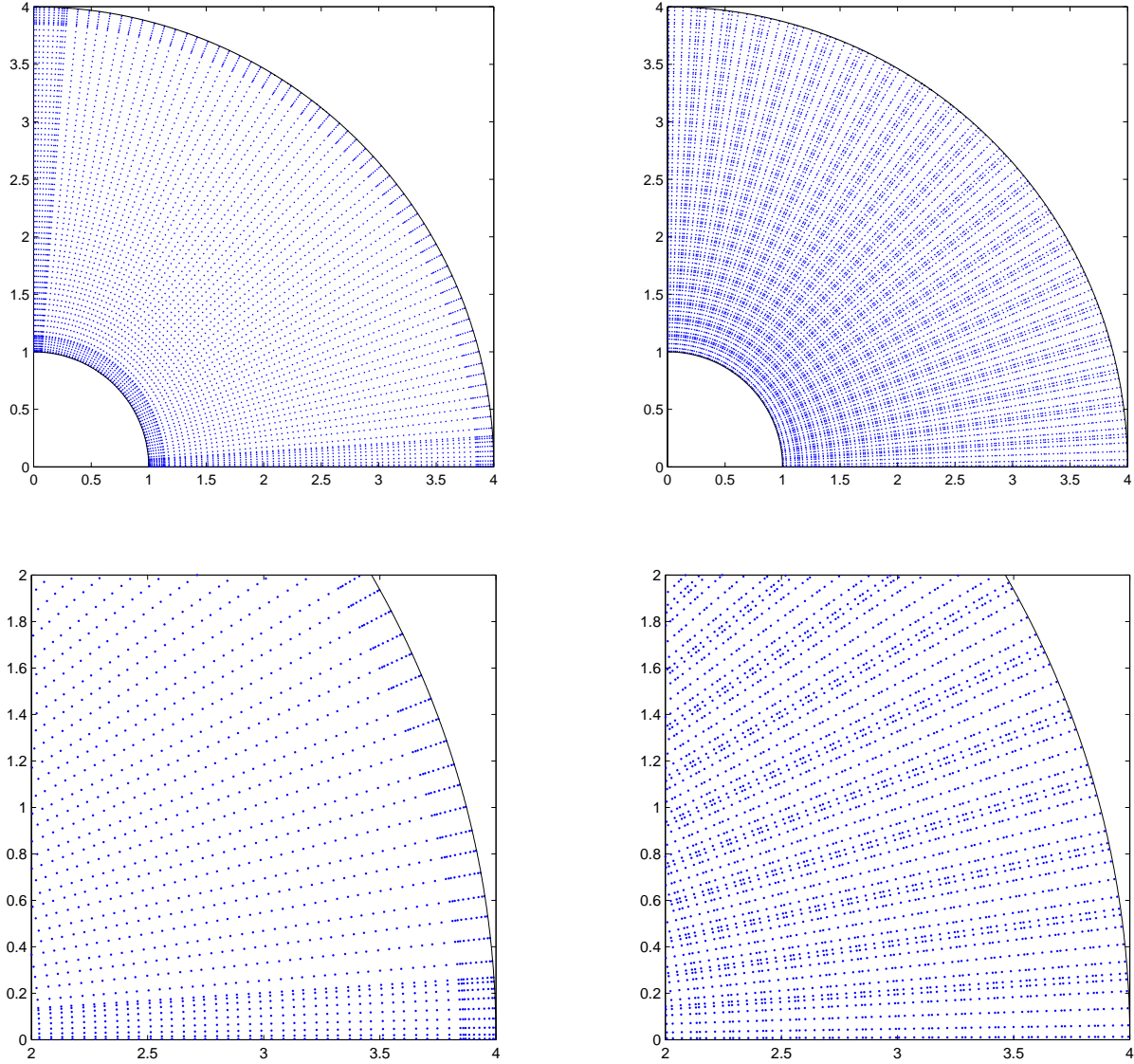


Figure 10: Poisson problem on a quarter of an annulus: distribution of integration points, in the case of basis function degree $p = q = 4$ in both parametric directions and a 25×25 control net, for the proposed new quadrature (top left) and the element-wise Gauss quadrature (top right). On the bottom, details of the bottom right corner of the plots above are reported.

interconnected by the so-called “transition” zones. Quadrature multi-patch can be easily treated, as well.

In this situation, the suggested solution is to perform integration considering each sub-patch individually, as if it was not connected to the others. Thus the proper internal quadrature rule has to be used for the internal elements of each sub-patch, while boundary integration has to be performed for the elements lying on the mesh borders as well as for transition zones. An example is given in Figure 11, where a mesh constituted by 6 different sub-patches is constructed as the tensor product of piecewise uniform and geometrically graded knot spans. The elements where boundary quadrature is in order are those adjacent to the black thick lines.

In particular, this possibility allows to perform integration on meshes that are composed of uniform zones (even of different mesh-sizes) and of non-uniform, geometrically graded zones (as described in the previous section), i.e., all the possible combinations of the quadrature rules considered in the present paper are possible. As a consequence, integration can be efficiently performed on a large variety of mesh situations, suitable to solve many of the problems typically tackled by means of tensor product NURBS-based IGA. An interesting example is reported in the next section.

We remark that this procedure is cost-effective only if the number of transition elements is significantly less than internal elements. If this is not the case, the macro-element quadrature presented in [21] is preferred.

4.3. Numerical solution of a reaction-diffusion problem with layers, on a suitable non-uniform mesh

In this section we make use of the non-uniform quadrature strategies discussed in the previous section, to compute the integrals necessary to solve the following reaction-diffusion problem defined on the bi-unit square $\Omega = [0, 1]^2$:

$$\begin{cases} -10^{-3} \cdot \Delta u + \frac{\partial u}{\partial x} = 1, & \forall x \in \Omega = [0, 1]^2, \\ u|_{\partial\Omega} = 0. \end{cases} \quad (4.2)$$

The exact solution of such a problem is a ramp of unit slope along the x -axis, showing two layers at $y = 0$ and $y = 1$, and a third, sharper layer at $x = 1$.

In order to solve this problem with a uniform mesh, a very small mesh size has to be selected in order to correctly capture the layers. Therefore, a non-uniform mesh, graded towards the

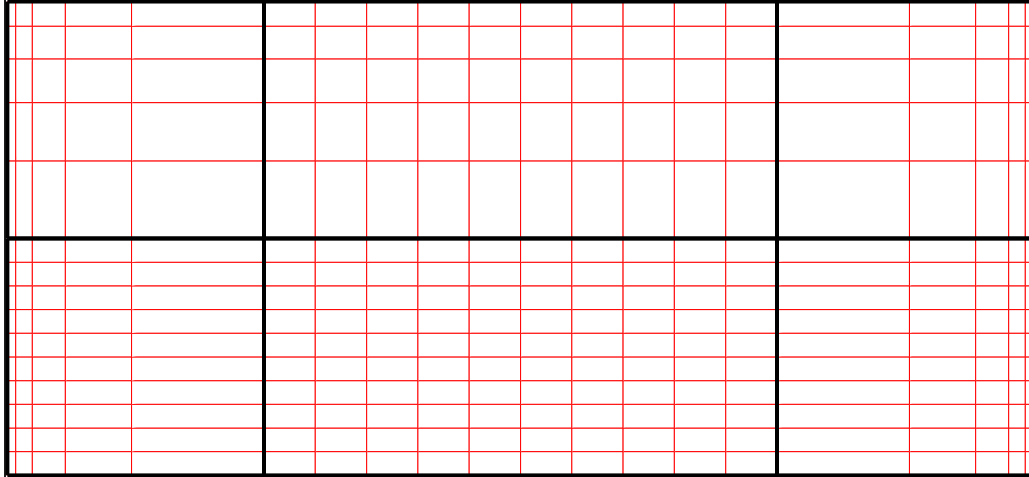


Figure 11: Quadrature multi-patch: example of a mesh consisting of 6 different sub-patches, constructed as the tensor product of piecewise uniform and geometrically graded knot spans. The elements where boundary quadrature is necessary are those adjacent to the black thick lines.

layers, is certainly preferred. Using the non-uniform quadrature strategies previously introduced, integration over a mesh like the one reported in Figure 12 is possible, allowing capturing the layers of the solution with a reasonable number of elements. The solution computed with a standard Galerkin IGA formulation (degree: $p = q = 3$, control net: 21×21) on such a mesh, using the new quadrature rules, is reported in Figure 12 as a color map, while in Figure 13 a 3D plot illustrates more clearly how the layers are reproduced by the numerical solution.

5. Summary and Conclusions

We have considered the development of efficient quadrature rules for NURBS-based Isogeometric Analysis. We have focused on rules for arrays that frequently arise in Finite Element Analysis, namely, mass, stiffness and advection matrices. We have reduced the quadrature problem to the exact integration of certain spaces of B-Splines in one dimension that have essential translation invariance and localization properties, and for this cases we have developed accurate rules for periodic B-Splines and B-Splines constructed for open knot vectors. Both uniform and geometrically scaled knot spacing have been considered. We have presented a simple and efficient algorithm for constructing the rules and we have illustrated its use on boundary value problems, including one whose solution possesses sharp boundary layers. The way to use the rule on domain consisting of

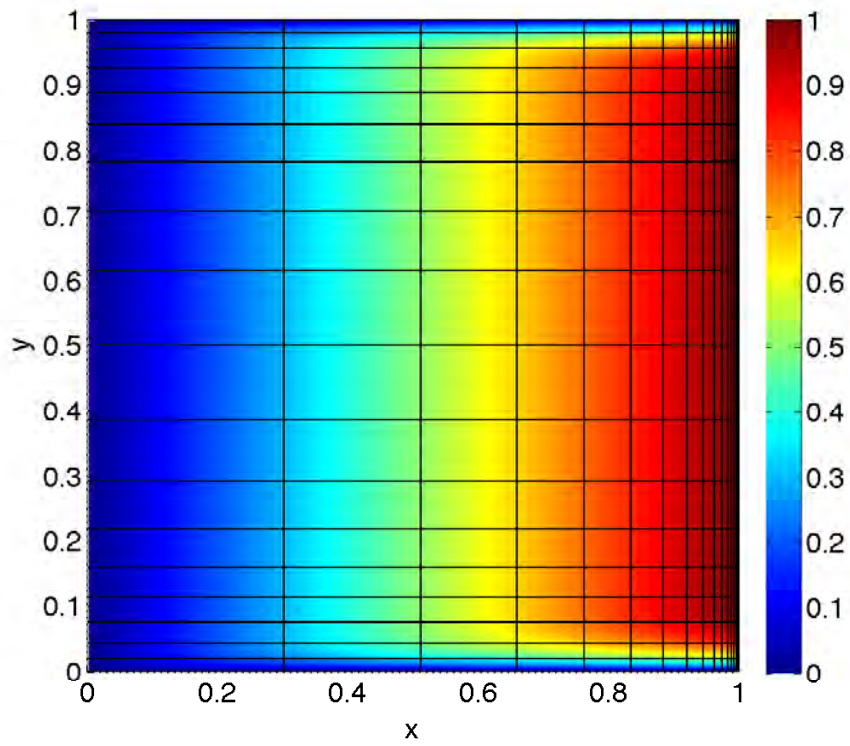


Figure 12: Reaction-diffusion problem with layers: adopted non-uniform mesh and color map of the corresponding numerical solution (degree: $p = q = 3$, control net: 21×21).

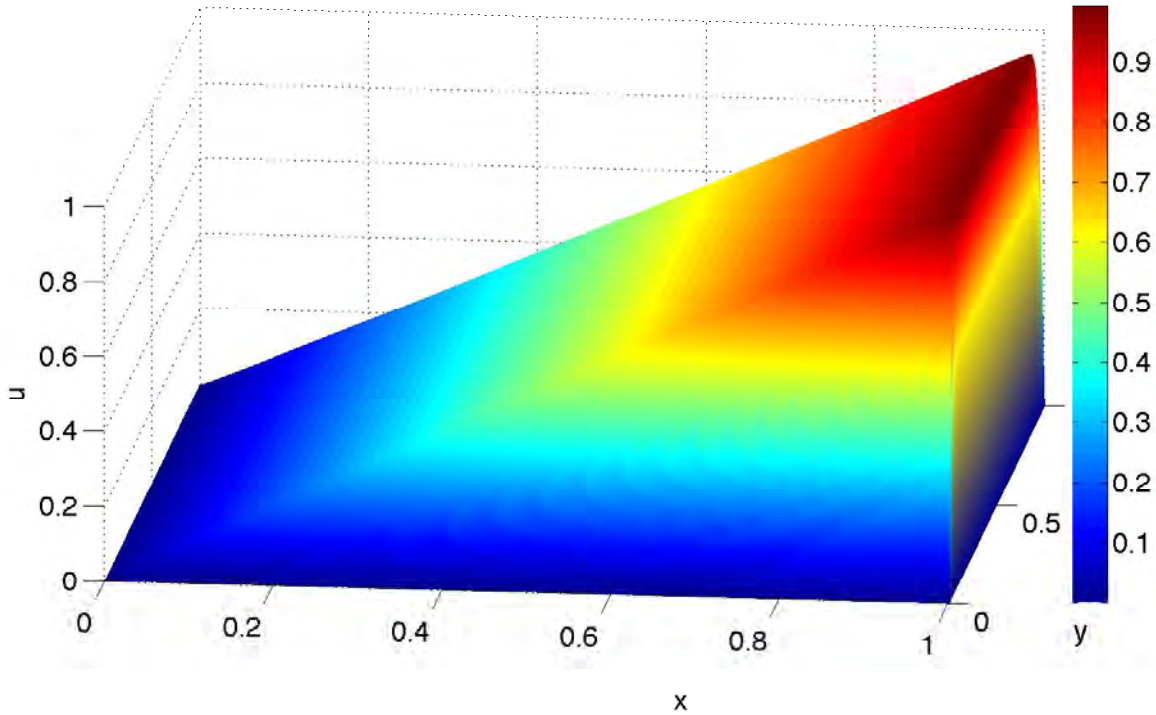


Figure 13: Reaction-diffusion problem with layers: 3D plot of the computed numerical solution (degrees: $p = q = 3$, control net: 21×21).

multiple patches has also been described. Our results indicate that the rules compare very favorably with optimal rules, which are at the very best difficult to obtain and in some cases almost impossible. The new rules are of course more efficient than Gauss quadrature repeated on knot spans. We believe this work takes another step forward in the development of specialized quadrature rules for NURBS-based Isogeometric Analysis. An obvious challenge is to develop rules for general non-uniform knot spacing. We plan to pursue this in future work.

Acknowledgments

F. Calabrò was partially supported by the GNCS project “Tecniche di quadratura e strutture di raffinamento nell’analisi isogeometrica”. T.J.R. Hughes was partially supported by the Office of Naval Research contract number N00014-08-0992, the Army Research Office contract number W911NF-10-1-0216, and SINTEF through the ICADA Project. F. Auricchio, A. Reali, and G. Sangalli were partially supported by the European Research Council through the FP7 Ideas Starting Grant n. 259229 *ISOBIO* and by the European Commission through the FP7 Factories of the Future project *TERRIFIC*. A. Reali and G. Sangalli were also partially supported by the European

Research Council through the FP7 Ideas Starting Grant n. 205004 *GeoPDEs* and by the Italian MIUR through the FIRB “Futuro in Ricerca” Grant RBFR08CZ0S. This support is gratefully acknowledged.

References

- [1] F. Auricchio, L. Beirão da Veiga, A. Buffa, C. Lovadina, A. Reali, G. Sangalli. A fully “locking-free” isogeometric approach for plane linear elasticity problems: A stream function formulation. *Comp. Meth. Appl. Mech. Engrg.*, **197**, 160–172, 2007.
- [2] F. Auricchio, L. Beirão da Veiga, T.J.R. Hughes, A. Reali, G. Sangalli. Isogeometric Collocation Methods. *Math. Mod. Meth. Appl. Sci.*, **20** (11), 2075–2107, 2010.
- [3] F. Auricchio, L. Beirão da Veiga, C. Lovadina, A. Reali. The importance of the exact satisfaction of the incompressibility constraint in nonlinear elasticity: mixed FEMs versus NURBS-based approximations. *Comp. Meth. Appl. Mech. Engrg.*, **199**, 314–323, 2010.
- [4] Y. Bazilevs, L. Beirão de Veiga, J.A. Cottrell, T.J.R. Hughes, G. Sangalli. Isogeometric analysis: approximation, stability and error estimates for h -refined meshes. *Mathematical Models and Methods in Applied Sciences*, **16**, 1–60, 2006.
- [5] Y. Bazilevs, V.M. Calo, J.A. Cottrell, T.J.R. Hughes, A. Reali, G. Scovazzi. Variational Multiscale Residual-based Turbulence Modeling for Large Eddy Simulation of Incompressible Flows. *Comp. Meth. Appl. Mech. Engrg.*, **197**, 173–201, 2007.
- [6] Y. Bazilevs, V.M. Calo, T.J.R. Hughes, Y. Zhang. Isogeometric fluid-structure interaction: theory, algorithms, and computations. *Comput. Mech.*, **43** (1), 3–37, 2008.
- [7] L. Beirão da Veiga, A. Buffa, J. Rivas, G. Sangalli. Some estimates for $h - p - k$ -refinement in isogeometric analysis, *to appear in Numer. Math.*, DOI: 10.1007/s00211-010-0338-z, 2010.
- [8] A. Buffa, C. de Falco, G. Sangalli. Isogeometric Analysis: new stable elements for the Stokes Equation. *to appear on Inter. J. Numer. Meth. Fluids*, DOI: 10.1002/fld.2337, 2010.
- [9] A. Buffa, J. Rivas, G. Sangalli, R. Vázquez. Isogeometric Discrete Differential Forms in Three Dimensions *to appear on SIAM J. Numer. Anal.*, DOI: 10.1137/100786708, 2011.

- [10] A. Buffa, G. Sangalli, R. Vázquez. Isogeometric analysis in electromagnetics: B-splines approximation. *Comp. Meth. Appl. Mech. Engrg.*, **199** (17-20), 1143–1152, 2010.
- [11] F. Calabrò and A. Corbo Esposito. An evaluation of Clenshaw-Curtis quadrature rule for integration w.r.t. singular measures. *JCAM*, **229**, 120–128, 2009.
- [12] H. Cheng, V. Rokhlin and N. Yarvin. Nonlinear optimization quadrature and interpolation. *SIAM J. Optim.*, **9**, (4), 901–923, 1999.
- [13] J.A. Cottrell, T.J.R. Hughes, Y. Bazilevs. *Isogeometric Analysis. Toward integration of CAD and FEA*. Wiley, 2009.
- [14] J.A. Cottrell, T.J.R. Hughes, A. Reali. Studies of Refinement and Continuity in Isogeometric Structural Analysis. *Comp. Meth. Appl. Mech. Engrg.*, **196**, 4160–4183, 2007.
- [15] J.A. Cottrell, A. Reali, Y. Bazilevs, T.J.R. Hughes. Isogeometric analysis of structural vibrations. *Comp. Meth. Appl. Mech. Engrg.*, **195**, 5257–5296, 2006.
- [16] C. de Falco, A. Reali, and R. Vázquez, *GeoPDEs: a research tool for isogeometric analysis of PDEs*, *Advances in Engineering Software*, **42**, 1020–1034, 2011.
- [17] J.A. Evans, Y. Bazilevs, I. Babuška, T.J.R. Hughes. n -width, sup-infs, and optimality ratios for the k -version of the isogeometric finite element method. *Comp. Meth. Appl. Mech. Engrg.*, **198**, 1726–1741, 2009.
- [18] H. Gomez, T. J. R. Hughes, X. Nogueira, V. M. Calo. Isogeometric analysis of the isothermal Navier-Stokes-Korteweg equations. *Comput. Methods Appl. Mech. Engrg.*, **199** (25-28), 1828–1840, 2010.
- [19] T.J.R. Hughes, J.A. Cottrell, Y. Bazilevs. Isogeometric analysis: CAD, finite elements, NURBS, exact geometry, and mesh refinement. *Comp. Meth. Appl. Mech. Engrg.*, **194**, 4135–4195, 2005.
- [20] T.J.R. Hughes, A. Reali, G. Sangalli. Duality and Unified Analysis of Discrete Approximations in Structural Dynamics and Wave Propagation: Comparison of p -method Finite Elements with k -method NURBS. *Comp. Meth. Appl. Mech. Engrg.*, **197**, 4104–4124, 2008.

- [21] T.J.R. Hughes, A. Reali, G. Sangalli. Efficient Quadrature for NURBS- based Isogeometric Analysis. *Comp. Meth. Appl. Mech. Engrg.*, **199**, 301–313, 2010.
- [22] S. Lipton, J.A. Evans, Y. Bazilevs, T. Elguedj, T.J.R. Hughes. Robustness of isogeometric structural discretizations under severe mesh distortion. *Comp. Meth. Appl. Mech. Engrg.*, **199**, 357–373, 2010.
- [23] J. Ma, V. Rokhlin and S. Wandzura. Generalized Gaussian Quadrature Rules for Systems of Arbitrary Functions. *SIAM Journal on Numerical Analysis*, **33** (3), 971–996, 1996.
- [24] A. Reali. An Isogeometric Analysis Approach for the Study of Structural Vibrations. *Journal of Earthquake Engineering*, **10** (s.i. 1), 1–30, 2006.
- [25] L.L. Schumaker. *Spline Functions: Basic Theory*. 3rd Edition, Cambridge Mathematical Library, Cambridge University Press, Cambridge, 2007.
- [26] The MathWorks. *Optimization Toolbox User's Guide*. Available online at <http://www.mathworks.com>, 2008.